The Final Steps of the Oppolzer Cyclization: Mechanism of the Insertion of Alkenes into Allylpalladium(II) Complexes

Diego J. Cárdenas,[a] Manuel Alcamí,[b] Fernando Cossío,[c] María Méndez,[a] and Antonio M. Echavarren*[a]

Abstract: We report here the results of a computational study on the the mechanism of the Oppolzer cyclization. These results lead us to conclude that the insertion of olefins in Pd–allyl complexes probably takes place directly from the η^3-allyl species. The presence of a phosphane ligand in the reagents plays the role of enhancing the electron density on the Pd atom; this makes the alkene moiety more reactive towards insertion by back-donation from the metal. The results also indicate that the configuration of the new stereogenic centers is fixed in the insertion of the alkene into the (η^3-allyl)palladium species.

Keywords: allylation · carbocycles · density functional calculations · insertion · palladium

Introduction

The palladium-catalyzed intramolecular reaction of allyl acetates with alkenes developed by Oppolzer is a powerful method for the formation of five- and six-membered carbocycles- and heterocycles.[1, 2] By analogy with the lithium- and magnesium-ene reactions,[1] the palladium-catalyzed process was originally suggested to take place by the pericyclic-type pathway outlined in Scheme 1.[1, 2] Accordingly, the allyl carboxylate **I** was proposed to react with a Pd^0 complex to form the (η^1-allyl)palladium(II) complex **II**, which then undergoes a palladium-ene reaction to give **III**. A β-hydride elimination would then produce 1,4-diene **IV** (R = H) or a 1,5-diene of type **V** if the elimination takes place through the side chain R.[1, 2] Dienes of type **V** can also be obtained by the intramolecular palladium-catalyzed transmetalation of allyl carboxylates with allylstannanes.[3]

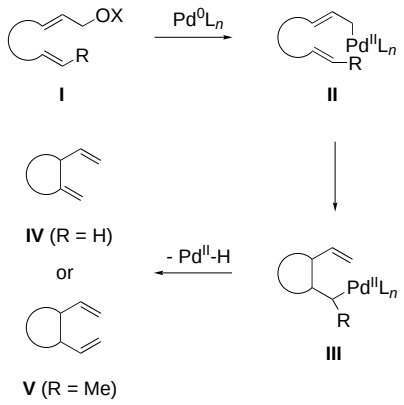

Scheme 1.

As a result of mechanistic work directed at the determination of the key intermediates in the Oppolzer reaction, we found that this cyclization proceeds through cationic (η^3-allyl)(η^2-alkene)palladium(II) complexes.[4] Thus, complexes, such as **2a** and **2b**, obtained from allyl trifluoroacetate **1** and a Pd^0 complex with PPh_3 as the ligand, undergo intramolecular insertion to give carbocycles **3a** and **3b** (Scheme 2). A related cationic complex **2c** with an aqua ligand failed to undergo the insertion reaction. Similarly, neutral (η^3-allyl)(η^2-alkene)palladium(II) complexes with trifluoroacetato or chloro ligands **2d**,**e** did not undergo the intramolecular insertion reaction. A complex similar to **2a**, but with the bulky phosphane PCy_3 as the ligand, also led to smooth cyclization, while P(*o*-Tol)$_3$, $AsPh_3$, $P(OPh)_3$, P(O-*i*Pr)$_3$, and $P(OMe)_3$ led to slower and/or less efficient cyclizations. On the other hand, diphosphanes or phenanthroline-type ligands led to palladium complexes that were not productive intermediates under both stoichiometric and catalytic conditions.[4]

[a] Prof. Dr. A. M. Echavarren, Dr. D. J. Cárdenas, Dr. M. Méndez
Departamento de Química Orgánica
Universidad Autónoma de Madrid
Cantoblanco, 28049 Madrid (Spain)
Fax: (+34) 913973966
E-mail: anton.echavarren@uam.es

[b] Dr. M. Alcamí
Departamento de Química
Universidad Autónoma de Madrid
Cantoblanco, 28049 Madrid (Spain)

[c] Prof. Dr. F. Cossío
Departamento de Química Orgánica I
Euskal Herriko Universitatea
P.K. 1072, 20008 San Sebastián-Donostia (Spain)

Supporting information for this article is available on the WWW under http://www.chemeurj.org or from the author: Atomic coordinates for structures of Schemes 6–8.

0947-6539/03/0901-0096 $ 20.00+.50/0 *Chem. Eur. J.* **2003**, *9*, No. 1

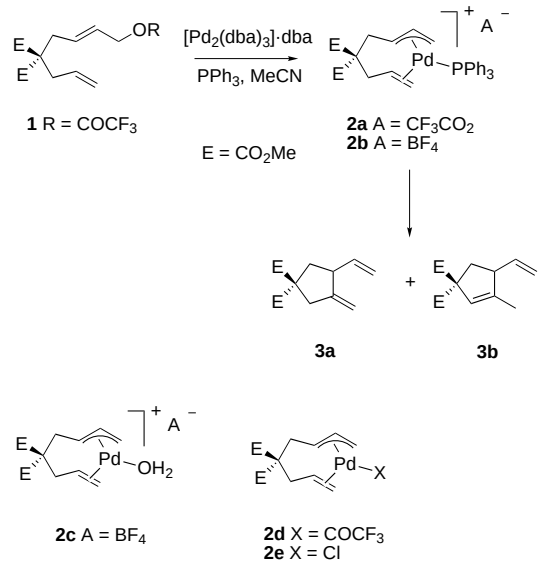

Scheme 2.

These results led to a reformulation of the catalytic cycle for the Oppolzer cyclization (Scheme 3). Thus, allylic carboxylates **I** oxidatively add to $[Pd^0L_n]$ to form complexes **VI**, which are in equilibrium with neutral (**VII**) and cationic (**VIII**) (η^3-allyl)palladium(II) complexes. Cationic complexes **VIII** then undergo intramolecular insertion, probably to give coordinatively unsaturated complexes **IX**, which finally give cycles **IV** or **V** by β-hydride elimination.

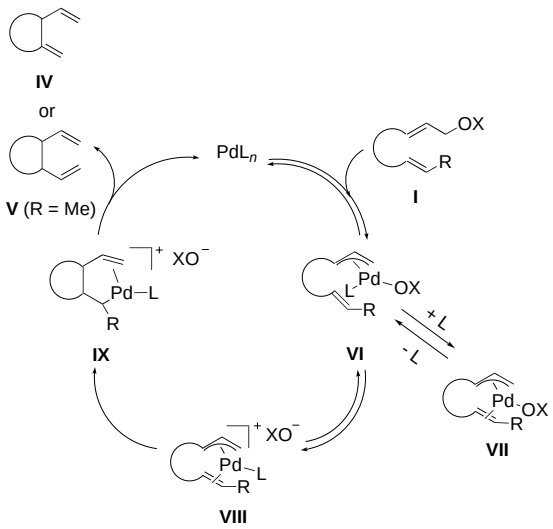

Scheme 3.

Cationic (η^3-allyl)palladium complexes[5] have also been shown to be key intermediates in the intermolecular insertion of alkenes into (η^3-allyl)palladium complexes.[6] Thus, Keim found that ethylene was inserted under mild conditions into complexes of this type that bear hemilabile P,O ligands.[6a] Similarly, Brookhart demonstrated that ethylene and methyl acrylate reacted with cationic (η^3-allyl)(PR_3)palladium complexes (R = Cy, *n*Bu) to give insertion products.[6b]

However, all these experimental results do not rigorously exclude the involvement of (η^1-allyl)palladium species,[7] formed from **VIII** by coordination with an additional ligand, as intermediates in the insertion of the alkene. Indeed, the intermolecular insertion of strained alkenes, such as norbornene, into (η^3-allyl)palladium hexafluoroacetylacetonate was proposed to proceed through (η^1-allyl)palladium intermediates.[8] In addition, the actual role played by the monodentate phosphane ligands in the insertion process was not understood.

With regards to the stereoselectivity of the C–C bond-forming step, the Oppolzer cyclization is known to favor formation of the more stable *trans*-dialkenyl five-membered cycles of type **V** in most cases.[1, 9] In this context, the other issue that remains to be addressed is the question of the reversibility of the C–C bonding event, since it has been proposed by Oppolzer that the formation of certain cycles might be under thermodynamic control.[1] Thus, the cyclization of malonate **4** gave a 1:1.7 mixture of *cis* **5a** and *trans* **5b** carbocycles after 5 h by the use of 5 mol% of $[Pd(PPh_3)_4]$ as the catalyst, while increasing the reaction time to 24 h and the loading of catalyst to 10% led to a 1:9 ratio of *cis* to *trans* stereoisomers (Scheme 4).[10] This apparent isomerization of

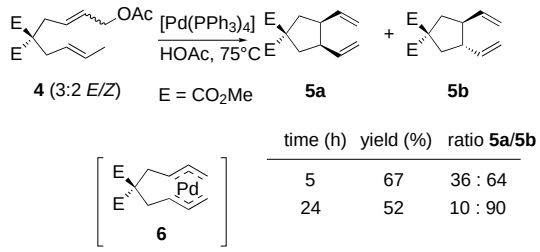

Scheme 4.

cis **5a** to more stable *trans* **5b** was explained as the result of a Cope rearrangement catalyzed by Pd^0, and proceeding through bis(η^3-allyl)palladium complex **6**. It is important to remark that this proposal is mechanistically quite different from the well-known Pd^{II}-catalyzed Cope-type rearrangement of 1,5-dienes.[11] In fact, the only precedent for the proposal of intermediates of type **6** in the isomerization of 1,5-dienes can be found in the recent finding by Yamamoto of such a transformation on substrates that bear electron-withdrawing groups, which facilitate their oxidative addition-type reaction to Pd^0.[12]

Because of the central role played by allylpalladium organometallic chemistry in current organic synthesis[13, 14] we decided to examine the insertion step in the Oppolzer cyclization in detail by means of high-level computational methods. We also address the question of the possible isomerization of *cis* and *trans* dienes of type **V**, because of its importance with regards to stereocontrol in the Oppolzer carbocyclization and heterocyclization reactions.

Computational Methods

The calculations were performed with the GAUSSIAN 98 series of programs.[15] The geometries of all complexes were optimized at the DFT level with the B3LYP hybrid functional.[16] The standard 6-31G(d) basis set

was used for C, H, O, and Cl and the LANL2DZ relativistic pseudopotential was used for Pd. Harmonic frequencies were calculated at the same level of theory to characterize the stationary points and to determine the zero-point energies (ZPE). Intrinsic reaction coordinate calculations (IRC) were performed to ensure that the transition states found for the insertion reaction from (η^1-allyl)palladium complexes actually connect the proposed reagents and products. Final energies were optimized, including ZPE energies scaled by the empirical factor of 0.9806.[17]

The bonding characteristics of the different local minima were analyzed by means of two different partition techniques: 1) the atoms in molecules (AIM) theory of Bader[18] and 2) the natural bond orbital (NBO) analysis of Weinhold et al.[19] The first approach is based on a topological analysis of the electron charge density, $\rho(\boldsymbol{r})$ and its Laplacian $\nabla^2\rho(\boldsymbol{r})$. More specifically, we have located the so-called bond critical points (bcp), that is, points at which $\rho(\boldsymbol{r})$ is minimum along the bond path and maximum in the other two directions. These points are associated with the positions of the chemical bonds. Then, at the bcp, $\rho(\boldsymbol{r})$ presents one positive curvature (l_3) and two negative ones (l_1, l_2). The ellipticity (e), defined as $e = l_1/l_2 - 1$, permits the characterization of the double or single character of the bond.[18] Charge concentration/depletion have been examined by means of the energy density $H(\boldsymbol{r})$, as introduced by Cremer et al.[20] In a similar fashion to $\nabla^2\rho(\boldsymbol{r})$, negative values of $H(\boldsymbol{r})$ are associated with covalent linkages, while positive values are usually associated with closed-shell interactions. The advantage of the use of $H(\boldsymbol{r})$ is that there are no exceptions to this interpretation when highly electronegative atoms (such as O) are involved in the bond. The NBO technique permits the description of the different bonds of the system in terms of the natural hybrid orbitals centered on each atom and also provides useful information on the charge distribution of the system.

The role of the solvation by $CHCl_3$ and MeCN was studied by means of the polarizable continuum model (PCM) of Tomasi.[21] Both single-point calculations on the structure optimized in the gas phase and reoptimization in the presence of solvent were performed on model cases.

Results and Discussion

To study the mechanism of the insertion step, we performed density functional theory (DFT) calculations with the B3LYP hybrid.[16] Two different families of complexes: [Pd^{II}-(η^3-allyl)(η^2-ethylene)] complexes (**Xa–d**) and [Pd^{II}(η^1-allyl)-(η^2-ethylene)] complexes (**XIa–d**) (Scheme 5) were used as models for the reagents in the insertion reaction. In complexes **XIa–d**, only the *cis* arrangement between the reacting allyl and alkene moieties was considered. The insertion products were also studied, including tricoordinate species (**XIIa–d**) and square-planar tetracoordinate ones (**XIIIa–d**) (Scheme 5). PH_3 was used as a model for phosphane ligands.

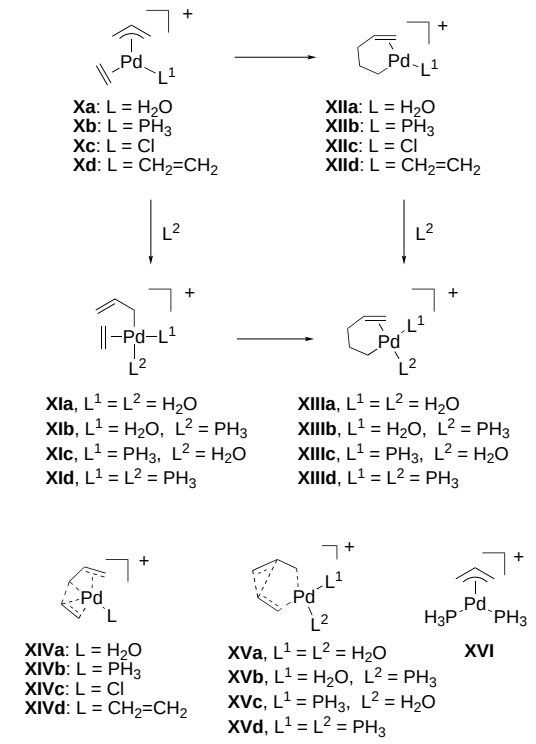

Scheme 5.

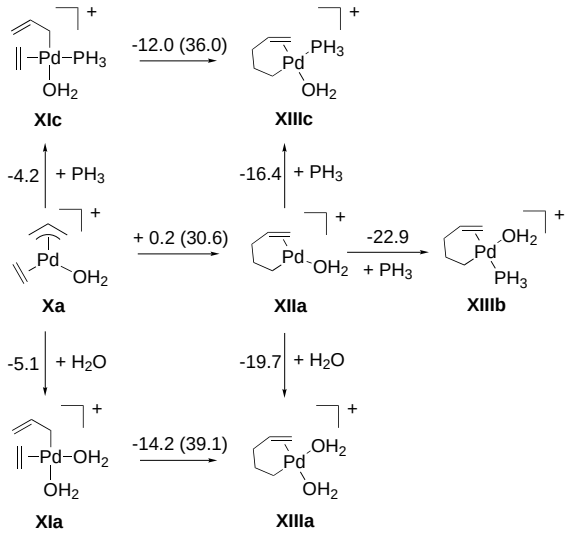

Scheme 6. Insertion pathways from aqua complex **Xa**. The values in parentheses correspond to the activation energies.

Insertion from (η^3-allyl)palladium complexes: The formation of the insertion products **XIIa–c** directly from η^3-allyl complexes **Xa–c** was shown to be slightly endothermic for the PH_3 and H_2O derivatives (0.2 kcal mol^{-1}) and exothermic for the chloride complex (-6.4 kcal mol^{-1}, Schemes 6 and 7). The corresponding transition states were located for all cases. The activation energy is significantly lower for the PH_3 complexes (22.5 kcal mol^{-1}) than for the chloride and aqua derivatives (28.2 and 30.6 kcal mol^{-1}, respectively), in agreement with the experimental conclusions.[4]

Complexes **Xa–c** show the usual structure for (η^3-allyl)Pd^{II} derivatives (Figure 1). The Pd–C(allyl) bond lengths are different depending on the ligand (PH_3, Cl, or H_2O). As expected, PH_3 exerts a higher *trans* influence relative to Cl^- and H_2O (2.284, 2.214, and 2.130 Å for the Pd–C bond *trans* to the ligand in **Xb**, **Xc**, and **Xa**, respectively) (Figure 1). No critical point was found in these complexes between Pd and the central allyl carbon, and only a ring critical point exists in that region. This is at variance with the results reported for (η^3-allyl)Pd complexes containing two equivalent ligands.[24a] The asymmetry of the structures considered in the present work can explain this difference. The most conspicuous feature of Figure 1 is that the ethylene ligand presents a different arrangement in the PH_3 complex. Thus, in **Xa** and **Xc**, the alkene lies perpendicular to the coordination plane, whereas in **Xb** both carbon atoms are coplanar to the Pd and P atoms. Both planar and perpendicular structures for the coordination of alkenes to d^8 metals have been observed.[22, 23]

0947-6539/03/0901-0098 $ 20.00+.50/0 *Chem. Eur. J.* **2003**, *9*, No. 1

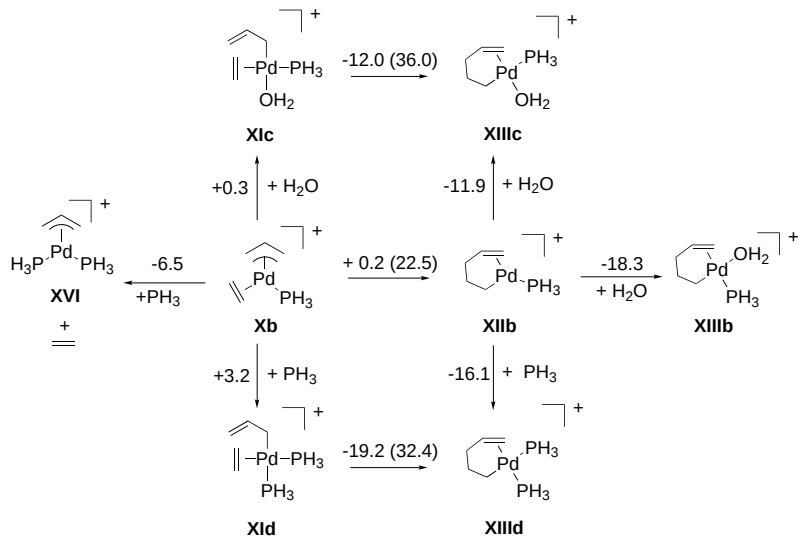

Scheme 7. Insertion pathways from phosphane complex **Xb**. The values in parentheses correspond to the activation energies.

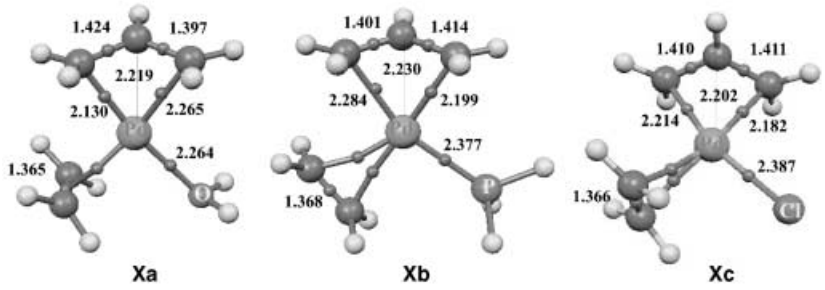

Figure 1. Molecular structures of (η^3-allyl)palladium complexes **Xa–c** showing relevant bond lengths [Å]. Dots between atoms represent the bond critical points found by analysis of the electron density.

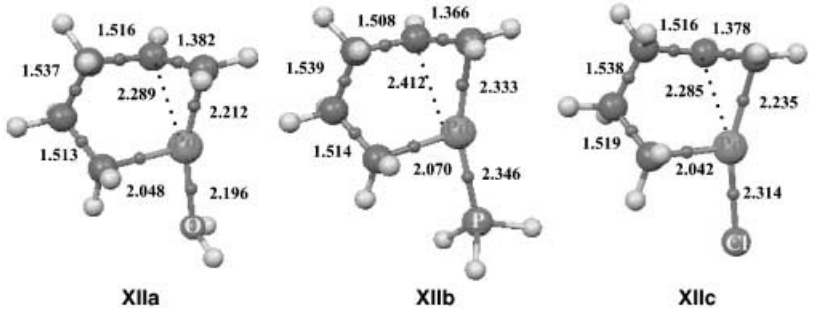

Figure 2. Molecular structures of the tricoordinate insertion products **XIIa–c** showing relevant bond lengths [Å]. Dots between atoms represent the bond critical points found by analysis of the electron density.

In our case, stable structures could not be found for either planar **Xa** or **Xc** or for perpendicular **Xb** (Figure 1).

The direct insertion reaction from these complexes would give rise to tricoordinate complexes **XIIa–c**, respectively. The PH_3, Cl, and H_2O ligands lie *trans* to the alkene fragment (Figure 2). This type of tricoordinate 14-electron Pd^{II} complexes are not easily formed by dissociation from tetracoordinate square-planar species; however, they have been proposed as intermediates in several reactions[24] in which they may be formed by mechanisms different from ligand dissociation, as in this case. Although the reactions of complexes **Xa,b** to **XIIa,b** are slightly endothermic (0.2 kcal mol^{-1}) (Schemes 6 and 7, and Figure 3), the fast incorporation of a ligand in the vacant coordination site (**XII** to **XIII** in Schemes 5–7), leads to a global exothermic process.

Late transition states (TS) for the insertion reactions from **Xa–c** (**XIVa–c**) have been observed for the three cases. The ethylene carbons lie in the coordination plane. NBO analysis shows that C–C bonds have already been formed and that a single bond critical point exists between the allyl ligand and the metal (Figure 4).

In complex **Xb**, the alkene is coplanar to the coordination plane of the allyl, being therefore closer to the TS geometry than aqua and chloride complexes **Xa–c**. An analysis of the electron density of **Xa–c** shows that, in complex **Xa**, only one bond critical point between ethylene and palladium exists, suggesting that there is no significant back-bonding from Pd to the alkene. On the other hand, in **Xb**, two bond critical points between the ethylene and Pd were located (Figure 1). These points correspond to two different Pd–C bonds with each of the alkene carbons, a situation that takes place when the metal fragment is relatively electron-rich. The greater σ-donor character of the phosphane with respect to water accounts for the fact that natural charge on Pd is lower in **Xb** than in **Xa** (0.47 and 0.60, respectively). The C–C bond in

L	E_a	ΔE
H_2O	30.6	+0.2
Cl	28.2	-6.4
$CH_2{=}CH_2$	22.7	-3.1
PH_3	22.5	+0.2

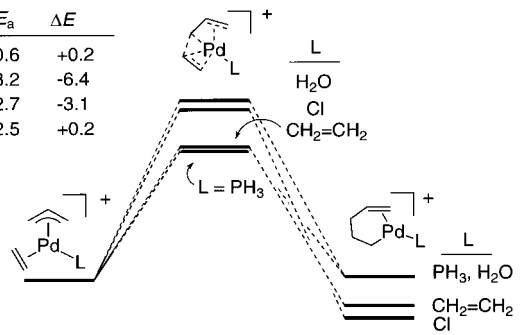

Figure 3. Energy profiles for the insertion reaction of (η^3-allyl)palladium complexes.

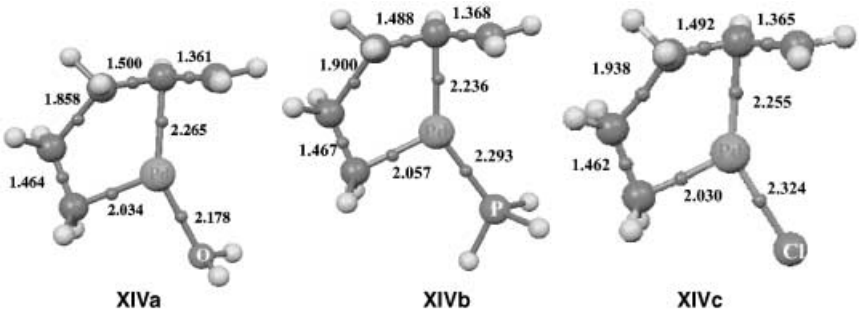

Figure 4. Transition states of the insertion reaction from (η^3-allyl)palladium complexes showing relevant bond lengths [Å].

the coordinated ethylene also reveals these differences: the C–C bond length is slightly longer in **Xb** than in **Xa** (1.368 vs. 1.365 Å), and there is a slight loss of double-bond character reflected in a lower ellipticity at the bond critical point (0.248 vs. 0.255) and in the deviation of ethylene atoms from planarity (H-C-C-H dihedral angle of 165.5 vs. 169.2°), leading to some degree of palladacyclopropane character in complex **Xb**.

NBO analysis (Table 1) gives a similar but more quantitative view of the charge distribution inside the complexes. Two conformations (coplanar or perpendicular) of the ethylene group with respect the allyl have been considered. As indicate above, for each complex, only one of them is a real minimum on the potential-energy surface (PES); the second one was obtained by fixing the geometry corresponding to the minimum and rotating the ethylene group by 90°. It can be seen that the planar position of the ethylene group favors the electronic charge transfer towards this group in all cases. Moreover, in agreement with the orbital analysis of similar Pt complexes,[25] the increase of electronic charge is the consequence of a better back-donation from a Pd orbital towards the π-antibonding orbital of ethylene, while the population of the π-bonding orbital of ethylene is not much affected by the conformation of the group (Table 1). The NBO analysis also permits the identification of those orbitals with the strongest interaction with the π-antibonding orbital of ethylene. In all cases, the most important interaction corresponds to the charge transfer from a lone pair on the Pd atom towards the π-antibonding orbital of ethylene. Table 1 also reveals that, in complexes **Xa** and **Xc**, the back-donation from Pd to ethylene is more important when the ethylene fragment is in a planar conformation, even though this is not the preferred one. The reason why the higher back-donation does not lead to a stabilization of the complex in these cases can be understood by looking at the origin of the charge. In complex **Xa** and **Xc**, the charge on the ligand (H_2O or Cl) is practically the same, independent of the conformation of the ethylene group. The extra charge transferred to ethylene comes from the allyl group. In the case of complex **Xb**, there is a larger charge transfer; however, more importantly, most of the charge comes from the PH_3 ligand, as expected on account of the lower electronegativity of phosphorus and the higher donor character of PH_3. The second-order perturbation analysis also reflects these differences, since in the case of complexes **Xa** and **Xc**, in the planar conformation there is an important charge transfer from a Pd–allyl σ-orbital toward the π-antibonding orbital of ethylene. This interaction is five times smaller in the case of complex **Xb**. Therefore, in the case of complexes **Xa** and **Xc**, a coplanar conformation of the ethylene group will reinforce the Pd–ethylene interaction, but it will also induce a depopulation of the allyl group and a weakening of the Pd–allyl interaction so that the overall effect is a destabilization of the complex with respect the perpendicular conformation.

It has to be noted that in complex **Xc**, AIM analysis shows the existence of two bond critical points between Pd and ethylene (see Figure 1); this reflects a donation to the π-antibonding orbital of ethylene similar to that of complex **Xb**, even though the ethylene is in a perpendicular position in complex **Xc**. NBO analysis shows that the population of the π-antibonding orbital is similar in both cases; however, in complex **Xc**, the large back-donation from Pd is a consequence of the neutral character of the complex. The rotation of ethylene to a planar position will further increase this back-donation, but it will deplete the allyl group and not the Cl ligand.

Table 1. NBO population analysis for complexes **Xa**, **Xb**, **Xc**, and **Xd**. Orbital interactions have been evaluated by means of a second-order perturbational analysis of the Fock matrix.

Complex	Ethylene conformation	Total charge				Orbital population		Orbital interactions [kcal mol^{-1}]
		Pd	allyl	ethylene	ligand	π (C=C)	π* (C=C)	
Xa	coplanar	0.591	0.201	0.103	0.106	1.783	0.118	Pd → π* (13.5)
								σ(Pd-allyl) → π* (9.7)
	perpendicular (minimum)	0.599	0.180	0.120	0.102	1.793	0.086	Pd → π* (14.4)
Xb	coplanar (minimum)	0.446	0.183	0.081	0.290	1.789	0.132	Pd → π* (14.4)
								σ(Pd-allyl) → π* (2.5)
	perpendicular	0.467	0.142	0.117	0.274	1.803	0.084	Pd → π* (14.0)
Xc	coplanar	0.558	0.041	0.022	−0.622	1.819	0.158	Pd → π* (15.8)
								σ(Pd-allyl) → π* (10.5)
	perpendicular (minimum)	0.582	−0.018	0.064	−0.628	1.812	0.114	Pd → π* (17.6)
Xd	coplanar (minimum)	0.569	0.205	0.091	0.135	1.803	0.105	Pd → π* (13.8)
								σ(Pd-allyl) → π* (1.1)
	perpendicular	0.556	0.212	0.112	0.120	1.815	0.080	Pd → π* (14.6)

0947-6539/03/0901-0100 $ 20.00+.50/0 *Chem. Eur. J.* **2003**, *9*, No. 1

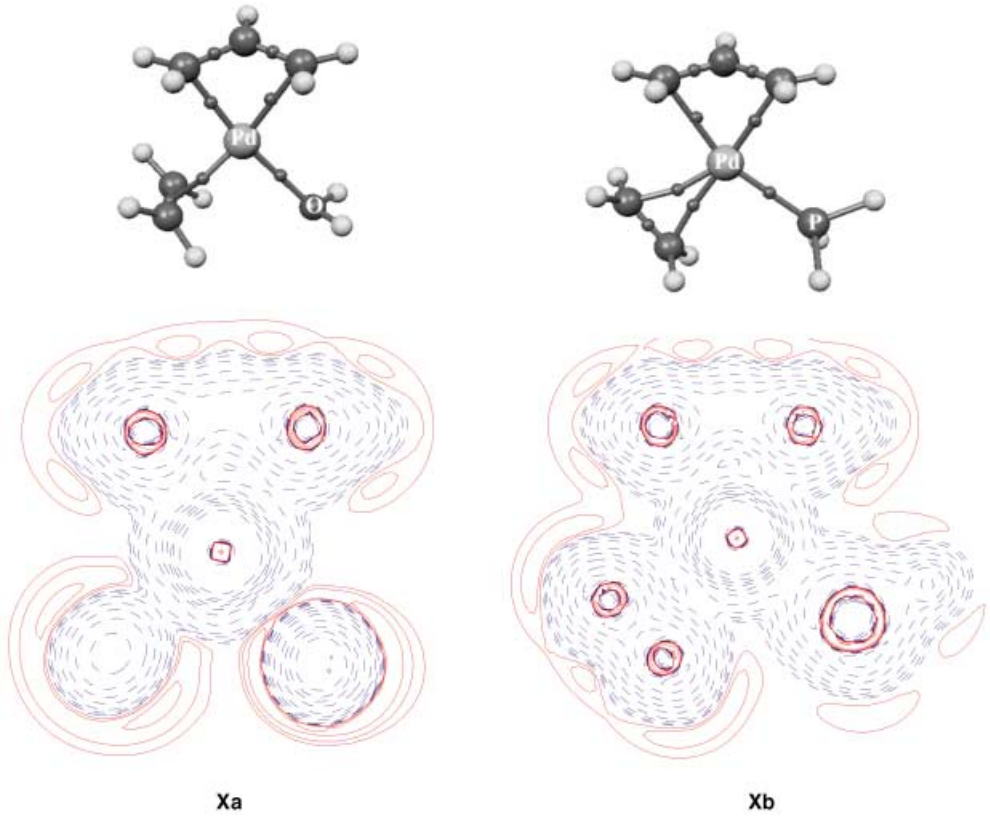

Figure 5. Energy density ($H(\boldsymbol{r})$) plots for a) **Xa** and b) **Xb** corresponding to the coordination planes. Solid and dashed lines correspond to positive and negative values of $H(\boldsymbol{r})$, respectively.

A closer look at the electron density of the cationic complexes **Xa–b** reveals further details. The different charge distribution between **Xa** and **Xb** is not only manifested in the C–C alkene bond length, but also in a larger charge delocalization in the alkene–allyl region in complex **Xb**, as it can be visualize in Figure 5. This figure also shows the σ-donor character of the phosphane,[26] for which the Pd–P bond region presents only negative values of the energy density (i.e. covalent character) in contrast to the Pd–O bond in **Xa**, in which a region of positive values of the energy density is found that corresponds to an interaction with higher ionic character.

Similar analysis of the corresponding transition states does not show significant differences in the structure and charge distributions among complexes **XIV**. As mentioned above, the new bond is already formed (Figure 4), and the Pd atom becomes linked to the central allyl carbon atom and to the terminal atom in the alkene. All these results lead to the conclusion that the differences found in the energy barriers are mainly caused by the favorable conformation in the initial reagent **Xb**, with the alkene ligand placed on the coordination plane. In addition, the higher *trans* influence of PH_3 weakens the $C_{ethylene}$–Pd bond in the starting complex that is cleaved in the insertion process, and makes it structurally closer to the transition state. In conclusion, **Xb** is more similar in structure, charge distribution, (and energy) to the corresponding TS than in the case of the aqua and chloride complexes **Xa** and **Xc**.

On the other hand, a recent work suggests that (η^3-allyl)bis(alkene)palladium complexes also readily undergo insertion reactions.[27] We decided to study complex **Xd**[28] as a model of such derivatives. Figure 6 shows different arrangements for both ethylene ligands. Two Pd–C bond critical points have been found for the ligand perpendicular to the coordination plane, which acts as a π-acceptor as well as a spectator ligand with a considerable *trans* influence. The other coordinated alkene shows the suitable conformation for the insertion process. The reaction is exothermic

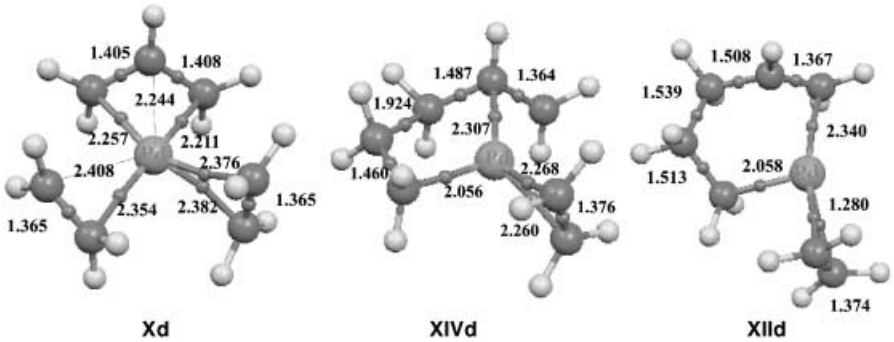

Figure 6. Stationary points for the insertion reactions of the chloride derivatives **Xd–XIId** showing relevant bond lengths [Å] and bond critical points.

  0947-6539/03/0901-0101 $ 20.00+.50/0

(-3.1 kcal mol^{-1}) and has an activation energy similar to that calculated for the PH_3 derivatives (22.7 kcal mol^{-1}), which is in agreement with the observed reactivity.[27]

A summary of the energy profiles for the insertion of ethylene into η^3-allyl–Pd are represented in Figure 3 as a function of the spectator ligand L.

Insertion from (η^1-allyl)palladium complexes: Coordination of an additional ligand to (η^3-allyl)Pd complexes may transform these derivatives into the (η^1-allyl)Pd (i.e. σ-allyl) species. In order to analyze the possible reaction paths, geometries were optimized for model complexes **XIa–d**, the corresponding insertion products **XIIIa–d**, and the transition states connecting both types of complexes (**XVa–d**) (Figure 7). We were able to compare the energetics of the insertion processes starting from η-allyl or σ-allyl species.

The inclusion of a water molecule as a second ligand with the formation of the η^1-allyl complexes was found to be exothermic for **Xa** and slightly endothermic for **Xb** (Schemes 6 and 7). However, it is important to note that, in the case of the interaction of **Xa** with H_2O, two different products were found: **XIa**, in which the water molecule enters as a ligand and the η^1-allyl complex is formed, and a second complex **Xa**·H_2O in which water is hydrogen-bonded to the aqua ligand and stabilizes the complex by 12.1 kcal mol^{-1} (Figure 8). Similarly, the interaction of **Xb** with water can lead to complex **XIc** or to a solvation complex, which is more stable by 4.6 kcal mol^{-1}. In the case of structure **XIb**, all our attempts to optimize evolved without activation barrier toward the solvation complex. When PH_3 is included as a second ligand in **Xb** to give **XId**, the reaction is endothermic (Scheme 7); however, more importantly, replacement of the olefin by the additional PH_3 to give complex **XVI**[28] (Scheme 5) is calculated to be an exothermic process by -6.5 kcal mol^{-1}.[29] Therefore, bidentate phosphanes are expected to displace the coordinated alkene and to inhibit the reaction, as observed experimentally.[4]

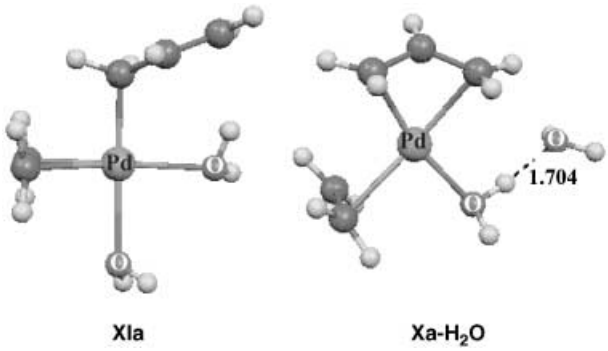

Figure 8. Molecular structures of **XIa** and **Xa**·H_2O.

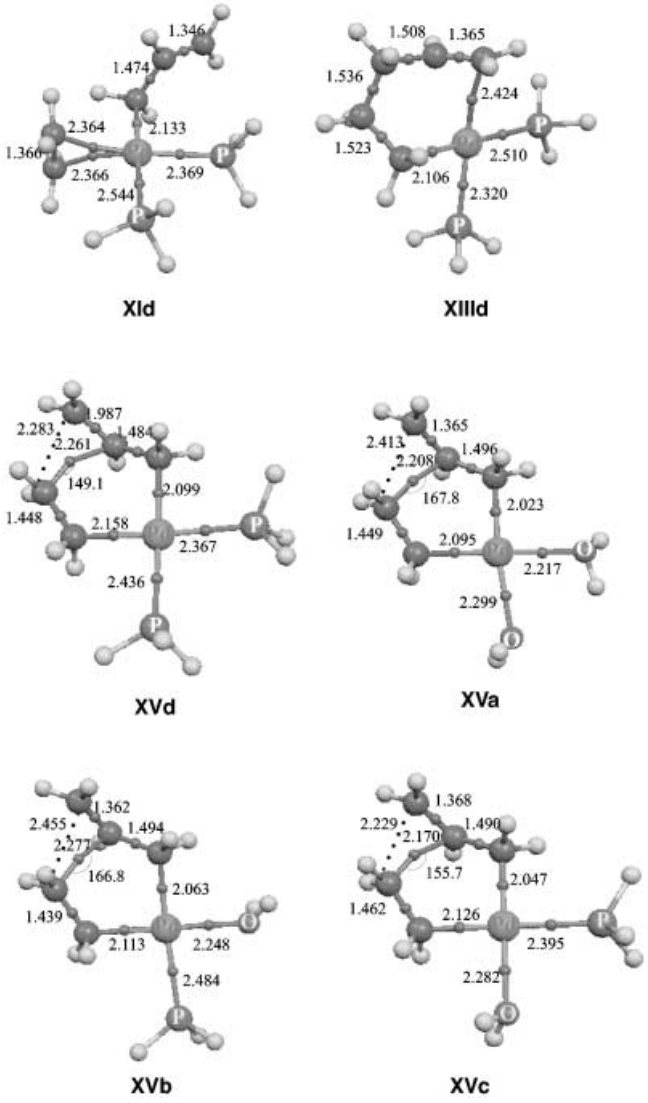

Figure 7. Molecular structures of the representative stationary points for the insertion from (η^1-allyl)palladium complexes. Relevant bond lengths [Å] and angles [°] are given in parentheses. Dots between atoms represent the bond critical points found by analysis of the electron density.

The transition states **XV** connecting complexes η^1-allyl complexes **XI** and insertion **XIII** were located and are shown in Figure 7. Interestingly, these structures are different from the usually proposed metallo-ene-type reaction mechanism. Both the terminal and the central carbons of the allyl ligand interact with the ethylene fragment. Starting from **XI**, the reaction can be envisaged as the shift of the Pd along the alkene to reinforce the σ-Pd–C bond with one of the ethylene carbons, which becomes appreciably pyramidalized. This incipient carbocation is stabilized by the C=C π bond of the allyl. In contrast, the other olefinic carbon shows less distortion compared to the reagent and interacts with the π electrons of the allyl C–C double bond. Analysis of the electron density shows a bond critical point between the π-cloud of the allylic C–C double bond and the olefinic carbon in all cases (Figure 7). It is interesting to note that this point is not at the same distance from both allylic carbons and its position depends on the ligands around Pd. In transition state **XVa**, the interaction mainly corresponds to the central allyl carbon, which gives a cationic character of a terminal atom. This character diminishes upon substitution of H_2O by PH_3 (**XVb** and **XVd**) to give more electron-rich metal fragments, and the critical point shifts to the terminal carbon, resulting in stabilization of the corresponding transition state. The angle between the terminal carbon of the ethylene, the bond critical point, and the central allyl carbon is related to the σ-C–C

0947-6539/03/0901-0102 $ 20.00+.50/0 *Chem. Eur. J.* **2003**, *9*, No. 1

bond that is being formed: the lower the value of the angle, the lower is the associated energy barrier.

Although these reactions (Schemes 6 and 7) are significantly exothermic, they present activation energies higher than those corresponding to the insertion of the alkene into the η^3-allyl derivatives. This strongly suggests direct insertion from these complexes. The lowest barrier corresponds to the monophosphane derivative **Xb**, followed by **Xa**, and the diphosphane complex **XId**. This result further supports the insertion from the η^3-complexes, since, as it has been mentioned before, bidentate phosphanes would displace the olefin ligand rather than generate η^1-species, thus inhibiting the insertion step. Again, the reactivity is enhanced by the increase of the electron density on the metal.

Since the complexes involved in these reactions have cationic character, we performed calculations that included solvent effects. Thus, the formation of **Xa** and **Xb**, and transition states **XIVa** and **XIVb** were recalculated in $CHCl_3$ and MeCN (dielectric constants 4.9 and 36.6, respectively).[30] The activation barriers differ by less than 2.5 kcal mol^{-1} (less than 7%) compared to the above-mentioned results. This indicates that the solvent effects are not relevant in this case.

Isomerization of the final 1,5-dienes promoted by Pd^0: The intramolecular insertion in complexes **Xa** and **Xb** is a slightly endothermic process. This suggests that, under the appropriate conditions, the formation of the C–C bond might be under thermodynamic control. However, coordination of a molecule of the solvent or an addition of phosphane may give complexes of type **XIIIb** and **XIIId**, respectively, in an exothermic process. In fact, in certain cases, the Oppolzer cyclization has been shown to be stereospecific with regard to the configuration of the alkene of the starting material.[9a]

A different equilibration process might operate in the proposed isomerization of 1,6-dienes of type **V**, whose final configuration might be thermodynamically controlled by means of a Pd^0-catalyzed Cope-type transformation through a bis(η^3-allyl)palladium complex of type **6** (Scheme 4).[10] To test this hypothesis, we decided to study the behavior of pure *cis* disulfone **7a**[31] in the presence of Pd^0.

The synthesis of **7a** was carried out by taking advantage of the *cis*-stereoselectivity of the palladium-catalyzed reaction of alkenyl allyl acetates, such as **8**, with organozinc reagents.[32] Thus, the reaction of **8** with Et_2Zn in the presence of [Pd(PPh$_3$)$_4$] as the catalyst, followed by iodolysis of the resulting alkylzinc species gave **9** (61%) (Scheme 8).[32] This iodide was homologated in four steps via nitrile **10**,[33] aldehyde **11**, and alcohol **12**, to give iodide **13**. Finally, elimination via the *o*-nitrophenylselenoxide[34] afforded pure *cis*-sulfone **7a**.

Disulfone **7a** was recovered unchanged when heated with 10% mol equivalents of [Pd(PPh$_3$)$_4$] in HOAc at 75 °C for 17 h, typical conditions for the Oppolzer cyclization.[1, 2] Similarly, no isomerization was observed with [Pd$_2$(dba)$_3$]·dba (5 mol%; dba = dibenzylideneacetone), PPh_3 (10 mol%), and LiCl (10 equiv) in aqueous DMF (80 °C, 17 h).[35] This result contradicts the proposal advanced for the result of Scheme 4.[10] Indeed, when the total isolated yields for **4a**/**4b** are taken into account, the result of the first entry translates to a 24% yield of *cis* **5a** and 43% yield of *trans* **5b**. The reaction at longer reaction times and higher catalyst loading, gives a 5% yield of **5a** and a 47% yield of **5b**. Hence, the increase of selectivity in that cyclization reaction can also be explained by the selective decomposition of **5a** at longer reaction times. Indeed, we have observed the slow decomposition of related substrates after they have been heated for long reaction times in the presence of Pd catalysts.

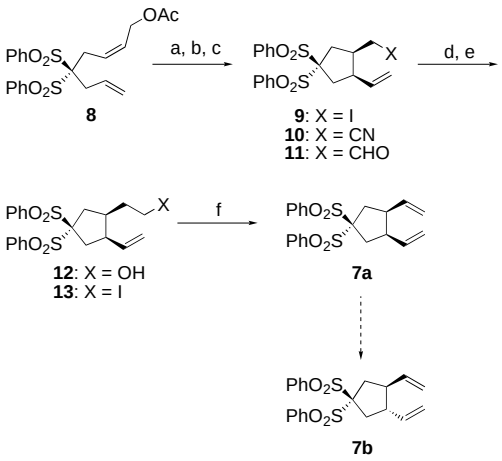

Scheme 8. Reagents and conditions: a) 61% (Ref. [32]); b) NaCN, DMF, 60 °C (90%); c) *i*Bu$_2$AlH (1.1 equiv), THF, −78 to 23 °C; aq. HCl (83%); d) $NaBH_4$, THF, 23 °C (99%); e) i) MsCl (1 equiv), Et_3N (1 equiv), CH_2Cl_2, 23 °C; ii) LiI (1.5 equiv), acetone, 40 °C (80%); f) *o*-$O_2NC_6H_4SeCN$ (1 equiv), $NaBH_4$ (3 equiv), DMF, 23 °C; H_2O_2 (excess), 23 °C (78%).

Conclusion

The computational study led us to conclude that the insertion of olefins in Pd–allyl complexes probably takes place directly from the η^3-allyl species. There is no need to propose a previous formation of η^1-allyl complexes. Therefore, this study supports the mechanism for the Oppolzer reaction outlined in Scheme 3. The presence of a phosphane ligand in the reagents plays the role of enhancing the electron density on the Pd atom; this makes the alkene moiety more reactive towards insertion by back-donation from the metal. A better back-donation from the metal, without affecting the charge density of the allyl group, favors a coplanar conformation of the allyl and alkene groups and the higher reactivity of the alkene moiety towards insertion. The use of bidentate phosphanes prevents the insertion from taking place, since the olefin is displaced from the coordination sphere, leading to a [Pd(η^3-allyl)(diphosphane)] complex as the stable species. The alternative reaction path by way of η^1-allyl complexes implies higher energy barriers. The transition states involved in these pathways differ from the proposed metallo-ene process, because significant bonding also takes place with the central carbon of the allyl even though the formation of the C–C bond proceeds through the terminus of the allyl ligand. An additional alkene ligand has an enhancement effect similar to that of PH_3.

  0947-6539/03/0901-0103 $ 20.00+.50/0

No isomerization of a *cis*-1,2-divinyl derivative to the more stable *trans* isomer was observed under typical conditions for Pd-catalyzed cyclizations. This result excludes equilibration of the final 1,5-dienes of type **V** by a Cope-type process, which indicates that the configuration of the new stereogenic centers is fixed in the insertion of the alkene into the (η^3-allyl)palladium species (**VIII** → **IX** in Scheme 3).

The overall mechanistic picture for the Oppolzer cyclization of allyl carboxylates is therefore consistent with that shown in Scheme 3.

Experimental Section

Iodide **9** was prepared from **8** (Scheme 8) according to the described procedure.[2e]

***cis*-2-[3,3-(Bisphenylsulfonyl)-5-ethenyl]cyclopentylacetonitrile (10)**: A solution of iodide **9** (1.60 g, 3.31 mmol) and KCN (323 mg, 4.96 mmol) in DMF (20 mL) was stirred for 14 h at 60 °C. The reaction mixture was diluted with Et_2O and washed 3 times with HCl (10%), dried over $MgSO_4$, and evaporated. The residue was purified by column chromatography to give known **10** (1.80 g, 90%) as a white solid. M.p. 148–150 °C (lit.:[2e] 157 °C); ^{1}H NMR (300 MHz, $CDCl_3$): $\delta = 8.13-8.04$ (m, 4H), 7.79–7.72 (m, 2H), 7.68–7.59 (m, 4H), 5.76 (ddd, $J = 17.0$, 10.4, 4.8 Hz, 1H), 5.19 (d, $J =$ 10.4 Hz, 1H), 5.14 (ddd, $J = 17.0$, 1.3, 1.2 Hz, 1H), 3.11–3.05 (m, 1H), 2.85–2.55 (m, 5H), 2.47–2.28 ppm (m, 2H); ^{13}C NMR (75 MHz, $CDCl_3$): $\delta = 136.20$, 135.44, 134.95, 134.63, 131.43, 128.92, 118.88, 92.96, 46.101, 39.88, 36.23, 35.42, 18.60 ppm.

***cis*-2-[3,3-(Bisphenylsulfonyl)-5-ethenyl]cyclopentylethanal (11)**: DibalH (1M in hexanes, 1.70 mL, 1.70 mmol) was added to a solution of nitrile **10** (622 mg, 150 mmol) in THF (30 mL) at −78 °C. The mixture was slowly warmed to 23 °C, and the solution was stirred 14 h at this temperature. The reaction mixture was then quenched with 10% HCl and extracted with Et_2O. The organic layer was washed once with HCl (10%) and once with brine, dried over $MgSO_4$, and evaporated. The residue was purified by column chromatography (EtOAc/hexane 3:7) to give **11** (520 mg, 83%) as a white solid. M.p. 135–137 °C; ^{1}H NMR (300 MHz, $CDCl_3$): $\delta = 9.72$ (s, 1H), 8.09–8.04 (m, 4H), 7.75–7.62 (m, 2H), 7.61–7.57 (m, 4H), 5.75 (ddd, $J = 17.0$, 10.1, 8.5 Hz, 1H), 5.06 (dd, $J = 10.1$, 1.6 Hz, 1H), 4.19 (db, $J =$ 17.0 Hz, 1H), 3.03–2.96 (m, 1H), 2.87 (dt, $J = 14.9$, 7.3 Hz, 1H), 2.74 (dd, $J = 15.6$, 6.9 Hz, 1H), 2.73–2.68 (m, 1H), 2.53 (d, $J = 7.7$ Hz, 2H), 2.51 (dd, $J = 15.7$, 6.9 Hz, 1H), 2.45 ppm (dd, $J = 15.4$, 7.8 Hz, 1H); ^{13}C NMR ($CDCl_3$, 75 MHz): $\delta = 200.69$, 136.71, 136.48, 135.74, 134.65, 134.56, 131.38, 131.22, 128.76, 128.68, 117.27, 93.48, 46.07, 44.59, 36.67, 36.61, 36.14 ppm; elemental analysis calcd (%) for $C_{21}H_{22}O_5S_2$: C 60.27, H 5.30, S 15.32; found: C 59.99, H 5.69, S 14.61.

***cis*-1,1-(Bisphenylsulfonyl)-3-ethenyl-4-(2-hydroxyethyl)cyclopentane (12)**: A solution of aldehyde **11** (200 mg, 0.47 mmol) and $NaBH_4$ (18 mg, 0.47 mmol) in THF (20 mL) was stirred for 4 h at 23 °C. The reaction mixture was quenched with H_2O and extracted with Et_2O. The organic layer was dried over $MgSO_4$, and the solvent was removed under reduced pressure to give **12** as colorless oil (195 mg, 99%). ^{1}H NMR (300 MHz, $CDCl_3$): $\delta = 8.04-7.96$ (m, 4H), 7.66–7.61 (m, 2H), 7.59–7.46 (m, 2H), 5.70 (ddd, $J = 16.8$, 10.2, 9.5 Hz, 1H), 5.03 (br d, $J = 10.2$ Hz, 1H), 4.94 (br d, $J =$ 16.8 Hz, 1H), 3.55 (t, $J = 6.5$ Hz, 2H), 2.87 (m, 1H), 2.77 (dd, $J = 15.6$, 7.6 Hz, 1H), 2.55–2.30 (m, 4H), 1.68 (br s, 1H, OH), 1.58 (m, 1H), 1.48 ppm (m, 1H); ^{13}C NMR ($CDCl_3$, 75 MHz): $\delta = 137.15$, 136.87, 135.93, 134.56, 134.45, 131.33, 131.24, 128.70, 128.62, 116.46, 93.84, 61.27, 48.83, 39.52, 36.81, 36.67, 33.02 ppm; FAB$^+$-HRMS calcd for $C_{21}H_{25}O_5S_2$ [M^++H]: 421.1143; found: 421.1141.

***cis*-1,1-(Bisphenylsulfonyl)-3-ethenyl-4-(2-iodoethyl)cyclopentane (13)**: Et_3N (69 μL, 0.76 mmol) and methanesulfonyl chloride (59 μL, 0.76 mmol) were added to a solution of alcohol **12** (321 mg, 0.76 mmol) in CH_2Cl_2 (20 mL) at 0 °C. The mixture was stirred for 2 h at 23 °C, and then the CH_2Cl_2 was removed under reduced pressure. LiI (153 mg, 1.14 mmol) and acetone (20 mL) were added, and the mixture was stirred overnight at 40 °C. The reaction mixture was extracted with Et_2O, washed with H_2O, and dried over $MgSO_4$. The residue was purified by column chromatography (hexane/EtOAc 8:2) to give **13** (320 mg, 80%) as a pale yellow solid. M.p. 100–102 °C; ^{1}H NMR (300 MHz, $CDCl_3$): $\delta = 8.12-8.02$ (m, 4H), 7.78–7.56 (m, 6H), 5.82 (ddd, $J = 16.7$, 10.2, 9.2 Hz, 1H), 5.06 (dd, $J = 10.2$, 2.2 Hz, 1H), 5.03 (dd, $J = 16.7$, 2.2 Hz, 1H), 3.54 (dt, $J = 11.3$, 6.5 Hz, 1H), 3.47 (dt, $J = 11.3$, 6.5 Hz, 1H), 3.04–2.87 (m, 1H), 2.80 (dd, $J = 15.0$, 7.3 Hz, 1H), 2.66–2.40 (m, 3H), 1.87–1.65 ppm (m, 2H); ^{13}C NMR ($CDCl_3$, 75 MHz): $\delta = 136.82$, 136.74, 134.72, 134.59, 131.38, 131.29, 128.84, 128.71, 116.96, 93.59, 46.34, 43.51, 36.95, 35.81, 34.03, 32.97, 4.27 ppm; EI-HMRS calcd for $C_{21}H_{23}IO_4S_2$: 530.0082; found: 530.0074.

***cis*-1,1-(Bisphenylsulfonyl)-3,4-diethenylcyclopentane (7a)**: A solution of *o*-$NO_2C_6H_4SeCN$ (90 mg, 0.27 mmol) and $NaBH_4$ (30 mg, 0.80 mmol) in DMF (4 mL) was stirred for 3 h at 23 °C and then cooled to 0 °C. A solution of the iodide **13** (140 mg, 0.27 mmol) in DMF (3 mL) was added, and the mixture was stirred at 23 °C for 19 h. The mixture was cooled to 0 °C, and H_2O_2 (30%, 5 mL) was added. The color of the reaction changed from red to yellow. The mixture was stirred at 23 °C for 6 h. After usual extractive work-up (Et_2O), the residue was purified by chromatography (hexane/EtOAc 7:3) to give **7a** as a white solid (85 mg, 78%). M.p. 78–80 °C; ^{1}H NMR (300 MHz, $CDCl_3$): $\delta = 8.07$ (br d, $J = 7.3$ Hz, 4H), 7.71 (m, 2H), 7.60 (m, 4H), 5.71 (ddd, $J = 16.9$, 10.5, 8.1 Hz, 2H), 5.01 (dd, $J = 10.5$, 1.6 Hz, 2H), 4.97 (dd, $J = 16.9$, 1.6 Hz, 2H), 3.01 (td, $J = 13.0$, 8.1 Hz, 2H), 2.67 (dd, $J = 15.4$, 7.3 Hz, 2H), 2.58 ppm (dd, $J = 15.8$, 7.3 Hz, 2H); ^{13}C NMR ($CDCl_3$, 75 MHz): $\delta = 137.38$, 136.07, 134.64, 134.51, 131.38, 131.32, 128.76, 128.68, 116.21, 93.87, 47.41, 36.92 ppm; FAB$^+$-HRMS calcd for $C_{21}H_{22}O_4S_2$ [M^++H]: 408.1037; found: 408.1028.

***trans* 7b**:[34b] This isomer showed distinct ^{1}H NMR signals for the alkenyl hydrogens: $\delta = 5.57$ (ddd, $J = 17.1$, 10.3, 6.9 Hz, 2H), 5.05 (dd, $J = 10.3$, 1.5 Hz, 2H), 4.99 ppm (dd, $J = 17.1$, 1.5 Hz, 2H).

Acknowledgement

We are grateful to the MCyT (Projects BQU2001-0193-C02-01 and BQU2000–245) for support of this research and to the MEC for a fellowship to M.M. We thank Drs. Enrique Gómez-Bengoa and Juan M. Cuerva for early contributions on the mechanism of the insertion reaction. We also acknowledge the Centro de Computación Científica (UAM) for computation time and Johnson Matthey PLC for a generous loan of $PdCl_2$.

[1] Reviews: a) W. Oppolzer, in *Comprehensive Organic Synthesis, Vol. 5* (Eds.: B. M. Trost, I. Fleming), Pergamon, Oxford, **1991**, Chapter 1.2; b) W. Oppolzer, in *Comprehensive Organometallic Chemistry II, Vol. 12* (Eds.: E. W. Abel, F. G. A. Stone, G. Wilkinson), Pergamon, Oxford, **1995**, Chapter 8.3; c) W. Oppolzer, *Angew. Chem.* **1989**, *101*, 39–53; *Angew. Chem. Int. Ed. Engl.* **1989**, *28*, 38–52; d) W. Oppolzer, *Pure Appl. Chem.* **1988**, *60*, 39–42; e) A. Heumann, M. Réglier, *Tetrahedron* **1995**, *51*, 975–1015.

[2] Additional references: a) E. Negishi, S. Iyer, C. J. Rousset, *Tetrahedron Lett.* **1989**, *30*, 291–294; b) R. Grigg, V. Sridharan, S. Sukirthalingam, *Tetrahedron Lett.* **1991**, *32*, 3855–3858; c) W. Oppolzer, J. Ruiz-Montes, *Helv. Chim. Acta* **1993**, *76*, 1266–1274; d) N. C. Ihle, C. H. Heathcock, *J. Org. Chem.* **1993**, *58*, 560–563; e) W. Oppolzer, F. Schröder, *Tetrahedron Lett.* **1994**, *35*, 7939–7942; f) M. Terakado, K. Murai, M. Miyazawa, K. Yamamoto, *Tetrahedron* **1994**, *50*, 5705–5718; g) K. Hiroi, K. Hirasawa, *Chem. Pharm. Bull.* **1994**, *42*, 786–791; h) E. Gómez-Bengoa, P. Noheda, A. M. Echavarren, *Tetrahedron Lett.* **1994**, *35*, 7097–7098; i) T. Doi, A. Yanagisawa, S. Nakanishi, K. Yamamoto, T. Takahashi, *J. Org. Chem.* **1996**, *61*, 2602–2603; j) W. Oppolzer, F. Schröder, S. Kahl, *Helv. Chim. Acta* **1997**, *80*, 2047–2057; k) W. Oppolzer, B. Stammen, *Tetrahedron* **1997**, *53*; 3577–3586; l) W. Oppolzer, D. L. Kuo, M. W. Hutzinger, R. Léger, J.-O. Durand, C. Leslie, *Tetrahedron Lett.* **1997**, *38*, 6213–6216; m) H. Yamada, S. Aoyagi, C. Kibayashi, *Tetrahedron Lett.* **1997**, *38*, 3027–3030; n) C. W. Holzapfel, L. Marais, *Tetrahedron Lett.* **1998**, *39*, 2179–2182; o) W. Oppolzer, F. Flachsmann, *Tetrahedron Lett.* **1998**, *39*, 5019–5022; p) W. Oppolzer, F. Flachsmann, *Helv. Chim. Acta* **2001**, *84*, 416–430; q) V. Michelet, J.-C. Galland, L. Charruault, M. Savignac, J.-P. Genêt, *Org. Lett.* **2001**, *3*, 2065–2067.

  0947-6539/03/0901-0104 $ 20.00+.50/0

[3] a) J. M. Cuerva, E. Gómez-Bengoa, M. Méndez, A. M. Echavarren, *J. Org. Chem.* **1997**, *62*, 7540–7541; b) For a review, see: M. Méndez, A. M. Echavarren, *Eur. J. Org. Chem.* **2002**, 15–28.

[4] E. Gómez-Bengoa, J. M. Cuerva, A. M. Echavarren, G. Martorell, *Angew. Chem.* **1997**, *109*, 795–797; *Angew. Chem. Int. Ed. Engl.* **1997**, *36*, 767–769.

[5] For a recent discussion on the structure of these complexes, see: C. Amatore, A. Jutand, G. Meyer, L. Mottier, *Chem. Eur. J.* **1999**, *5*, 466–473.

[6] a) S. Mecking, W. Keim, *Organometallics* **1996**, *15*, 2650–2656; b) G. M. DiRenzo, P. S. White, M. J. Brookhart, *Am. Chem. Soc.* **1996**, *118*, 6225–6234.

[7] Well-characterized (η^1-allyl)palladium(II) complexes have been shown to react with alkenes to yield 3+2 cycloadducts instead of insertion derivatives: H. Kurosawa, A. Urabe, K. Miki, N. Kasai, *Organometallics* **1986**, *5*, 2002–2008, and references cited therein.

[8] a) R. P. Hughes, J. Powell, *J. Organomet. Chem.* **1973**, *60*, 387–407; b) R. P. Hughes, J. Powell, *J. Organomet. Chem.* **1973**, *60*, 409–425.

[9] a) However, formation of 3,4-divinylpyrrolidines was dependent on the configuration of the alkene of the starting material: W. Oppolzer, J. M. Gaudin, M. Bedoya-Zurita, J. Hueso-Rodríguez, J. M. Raynham, C. Robyr, *Tetrahedron Lett.* **1988**, *29*, 4709–4712; b) The Rh^I-catalyzed process favors formation of *cis*-3,4-divinylpyrrolidines: W. Oppolzer, A. Fürstner, *Helv. Chim. Acta* **1993**, *76*, 2329–2337.

[10] a) W. Oppolzer, J. M. Gaudin, R. E. Swenson, J.-P. Barras, 3er Congres National de la Societé Française de Chimie, Nice (France), September 5, **1988** (cited in ref. [1c]); b) Starting from the trifluoroacetate, instead of the acetate **4**, the palladium-catalyzed cyclization ($[Pd_2[dba]_3]\cdot$ dba (10 mol%), PPh_3 (20 mol%), toluene under reflux, 16 h afforded selectively **4b** in 95% yield.

[11] a) L. E. Overman, *Angew. Chem.* **1984**, *96*, 565–573; *Angew. Chem. Int. Ed. Engl.* **1984**, *23*, 579–586; b) R. P. Lutz, *Chem. Rev.* **1984**, *84*, 205–247; c) L. E. Overman, A. F. Renaldo, *J. Am. Chem. Soc.* **1990**, *112*, 3945–3949.

[12] H. Nakamura, H. Iwama, M. Ito, Y. Yamamoto, *J. Am. Chem. Soc.* **1999**, *121*, 10850–10851.

[13] J. Tsuji, *Palladium Reagents and Catalysts*; Wiley, Chichester, **1995**.

[14] Insertion of alkynes into cationic (η^3-allyl)palladium complexes may be involved in the palladium-catalyzed benzannulation of alkynes with allyl tosylates: N. Tsukada, S. Sugawara, Y. Inoue, *Org. Lett.* **2000**, *2*, 655–657.

[15] M. J. Frisch, G. W. Trucks, H. B. Schlegel, G. E. Scuseria, M. A. Robb, J. R. Cheeseman, V. G. Zakrzewski, J. A. Montgomery, Jr., R. E. Stratmann, J. C. Burant, S. Dapprich, J. M. Millam, A. D. Daniels, K. N. Kudin, M. C. Strain, O. J. Farkas, J. Tomasi, V. Barone, M. Cossi, R. Cammi, B. Mennucci, C. Pomelli, C. Adamo, S. Clifford, J. Ochterski, G. A. Petersson, P. Y. Ayala, Q. Cui, K. Morokuma, D. K. Malick, A. D. Rabuck, K. Raghavachari, J. B. Foresman, J. Cioslowski, J. V. Ortiz, A. G. Baboul, B. B. Stefanov, G. Liu, A. Liashenko, P. Piskorz, R. Komaromi, R. L. Gomperts, D. J. Martin, T. Fox, M. A. Keith, C. Y. Al-Laham, I. Peng, A. Nanayakkara, M. Challacombe, P. M. W. Gill, B. Johnson, W. Chen, M. W. Wong, J. L. Andres, C. Gonzalez, M. Head-Gordon, E. S. Replogle, J. A. Pople, Gaussian 98, Revision A.9, Gaussian, Pittsburgh, PA, **1998**.

[16] a) A. D. Becke, *Phys. Rev. A* **1988**, *38*, 3098–3100; b) C. Lee, W. Yang, R. G. Parr, *Phys. Rev. B* **1988**, *37*, 785–789.

[17] A. P. Scott, L. Radom, *J. Phys. Chem.* **1996**, *100*, 16502–16513.

[18] R. F. Bader, W. *Atoms in Molecules. A Quantum Theory*, Clarendon, Oxford, **1990**.

[19] A. E. Reed, L. A. Curtiss, F. Weinhold, *Chem. Rev.* **1988**, *88*, 899–926.

[20] D. Cremer, E. Kraka, *Angew. Chem.* **1984**, *96*, 612–614; *Angew. Chem. Int. Ed. Engl.* **1984**, *23*, 62–64.

[21] J. Tomasi, M. Persico, *Chem. Rev.* **1994**, *94*, 2027–2094.

[22] J. P. Collman, L. S. Hegedus, J. R. Norton, R. G. Finke, *Principles and Applications of Organotransition Metal Chemistry*, University Science Books, Mill Valley, CA, **1987**, pp. 41–42.

[23] In palladium complexes with the allyl and alkenyl tethered by a chain, the planar or perpendicular arrangements might be controlled by conformational constraints. Thus, both arrangements have been found in solution and in the solid state for a cationic complex of this type: M. E. Kraft, M. Sugiura, K. A. Aboud, *J. Am. Chem. Soc.* **2001**, *123*, 9174–9175. See also: R. Ciajolo, M. A. Jama, A. Tuzi, A. Vitagliano, *J. Organomet. Chem.* **1985**, *295*, 233–238.

[24] a) A. L. Casado, P. Espinet, *J. Am. Chem. Soc.* **1998**, *120*, 8978–8985; b) A. L. Casado, P. Espinet, A. M. Gallego, *J. Am. Chem. Soc.* **2000**, *122*, 11771–11782.

[25] K. Miki, K. Yamatoya, N. Kasai, H. Kurosawa, A. Urabe, M. Emoto, K. Tatsumi, A. Nakamura, *J. Am. Chem. Soc.* **1988**, *110*, 3191–3198.

[26] Phosphanes PX_3 may also present important π-accepting character. In the case of PH_3, the π contribution has been estimated to represent 25% of the σ-donor contribution: a) Ó. González-Blanco, V. Branchandell, *Organometallics* **1997**, 16, 5556–5562; b) D. Woska, A. Prock, W. P. Giering, *Organometallics* **2000**, *19*, 4629–4638.

[27] K. L. Bray, J. P. H. Charmant, I. J. S. Fairlamb, G. C. Lloyd-Jones, *Chem. Eur. J.* **2001**, *7*, 4205–4215.

[28] Complex **Xd** has been previously studied: a) K. J. Szabó, *Organometallics* **1996**, *15*, 1128–1133; b) S. Sakaki, K. Takeuchi, M. Sugimoto, *Organometallics* **1997**, *16*, 2995–3003.

[29] Alkyl-substituted alkenes are expected to be replaced more easily. See, for example: H. Kurosawa, N. Asada, A. Urabe, M. Emoto, *J. Organomet. Chem.* **1984**, *272*, 321–329.

[30] Other usual solvents for these reactions have similar dielectric constants (toluene 2.38, and acetic acid 6.15).

[31] At the semiempirical PM3 level, **7a** is calculated to be 1.65 kcal mol^{-1} less stable than its *trans* isomer ($H_f = -18.35$ kcal mol^{-1} (**7a**), $H_f = -20.00$ kcal mol^{-1} (**7b**)]. The same energy difference (1.68 kcal mol^{-1}) was calculated between **4a** ($H_f = -136.86$ kcal mol^{-1}) and **4b** (-138.54 kcal mol^{-1}).

[32] W. Oppolzer, F. Schröder, *Tetrahedron Lett.* **1994**, *35*, 7939–7942.

[33] Reaction of the intermediate alkylzinc species with TsCN has been reported to afford the nitrile **10**.[32] However, this protocol proved to be less satisfactory than the two-step procedure used in our work.

[34] P. A. Grieco, M. Nishiwaza, S. D. Burke, N. Marinovic, *J. Am. Chem. Soc.* **1976**, *98*, 1612–1613.

[35] a) An intramolecular Pd-catalyzed Oppolzer reaction provided a mixture of **7a** and its *trans* isomer **7b**, thus allowing for the NMR determination of any **7b** that could have been formed from **7a**. Pure **7b** has been obtained by an intramolecular Pd-catalyzed coupling; b) M. Méndez, J. M. Cuerva, E. Gómez-Bengoa, D. J. Cárdenas, A. M. Echavarren, *Chem. Eur. J.* **2002**, *8*, 3620–3628.

Received: July 17, 2002 [F4255]